First principles resonance widths for Li near an Al(001) surface: Predictions of scattered ion neutralization probabilities

Keith Niedfeldt and Emily A. Carter[a)]
Department of Chemistry and Biochemistry, University of California, Los Angeles, California 90095-1569

P. Nordlander
Department of Physics and Rice Quantum Institute, Rice University, Houston, Texas 77251

(Received 22 March 2004; accepted 7 June 2004)

By combining a first-principles periodic density functional theory calculation of adsorbate resonance widths with a many-body dynamical theory of charge transfer, we assess charge-transfer rates for ions scattering off metal surfaces. This goes beyond previous approaches, which have been limited to modeling the surfaces with either static potentials or finite clusters. Here we consider Li^+ scattering from an Al(001) surface. We show how the Li $2s$ orbital hybridizes with metal valence bands, near the surface, increasing the width of the $2s$ energy level. This in turn affects the charge-transfer rates between the ion and the metal surface. Our predictions for Li^+-Al(001) scattering yield the correct angular dependence of the fraction of neutral Li atoms formed when compared to experiment. © *2004 American Institute of Physics.* [DOI: 10.1063/1.1777218]

I. INTRODUCTION

Investigations of atomic species scattering from surfaces have advanced our understanding of charge-transfer processes. In the hyperthermal scattering energy regime, where charge transfer between the atom and the surface occurs at relatively large distances, it is sufficient to represent the surface with a jellium description,[1] because atomically resolved chemical interactions between the atom and the surface are negligible. In this case, the electron potential barrier between the atom and the surface can be constructed by superposing a classical image contribution from the surface with the effective electronic potential for the atom. Several nonperturbative methods have been developed for the calculation of the tunneling rates between atoms and surfaces using a jellium model.[2–4] By contrast, in the low-energy ion scattering regime in which charge transfer occurs close to the surface, the jellium representation begins to fail[5–7] due to the need to incorporate a fully atomistic model of the surface.

Recent work has moved beyond the conventional jellium approaches. The coupled angular mode method[3] has been modified to successfully incorporate arbitrary static potentials for the metal surface.[8] New methods that formally calculate short-ranged chemical interactions between the scattering species and the surface atoms have been implemented.[9,10] Here we improve upon finite cluster local density approximation (LDA) (Ref. 9) and tight binding[10] models by using a periodic slab density functional theory (DFT) (Refs. 11 and 12) description. This method explicitly accounts for short-ranged chemical interactions, while avoiding cluster size effects.

Here we study the effects of one-electron resonant tunneling events, i.e., resonant ionization and resonant neutralization. When the scattering species is near the surface, species-surface electron tunneling can occur repeatedly in a dynamical exchange of charge. Using our first-principles calculations of the lifetimes of the atomic resonance states as a function of distance, we then calculate the charge-transfer behavior using a nonequilibrium time-dependent Hamiltonian. This Anderson Hamiltonian, whose parameters are taken as much as possible from our periodic DFT calculations, is then used to extract charge-transfer and neutralization probabilities from scattering trajectories.[13]

As an atom approaches a surface, its energy levels shift and broaden. Our postelectronic structure method to determine energy level widths is described in Sec. II. In Sec. III, we describe the DFT calculation of the broadening of the Li $2s$ level outside the Al(001) surface. An analysis of these energy level widths is presented in Sec. IV. Section V describes the dynamical method we use to relate the postcollision population to the precollision population. In Sec. VI we calculate the Li^+ neutralization probability as a function of exit angle, finding good agreement with experiment[14] and previous theory.[15] We conclude in Sec. VII.

II. ATOMIC ENERGY LEVEL WIDTHS

The Taylor-Nordlander[9] method for calculating the widths of atomic energy levels near metal clusters is adapted here to periodically infinite solids. This is accomplished by calculating the projected density of states (PDOS) for an atom near the extended metal surface.

$$\mathrm{PDOS}(l,E)=2\pi\sum_m |\langle\phi_m|\phi_l\rangle|^2\delta(E-E_m). \quad (1)$$

This PDOS is a function of the energy E and the orbital l onto which we are projecting. The interacting system [for example, Li/Al(001) described in Sec. III] is composed of m Kohn-Sham (KS) orbitals calculated from DFT. In Eq. (1) we determine the overlap between the KS orbital of the interacting system (ϕ_m) and the KS orbital of the isolated scattering species onto which we are projecting (ϕ_l). E_m are the energy levels of the interacting system. For a periodic system, we expand ϕ_m and ϕ_l in Eq. (1) in a plane wave basis, obtaining

a)Electronic mail: eac@chem.ucla.edu

$$\mathrm{PDOS}(l,E)=2\pi\sum_m \left|\left\langle \sum_k w_k \sum_{\vec{G}} c_{(\vec{G}+\vec{k}),m} \times e^{i(\vec{G}+\vec{k})\cdot\vec{r}} \left| \sum_{\vec{G}'} c_{\vec{G}',l} e^{i\vec{G}'\cdot\vec{r}} \right\rangle \right|^2 \times \delta(E-E_{m,k}). \quad (2)$$

Here the plane wave expansion requires a summation over k special k-points in the first Brillouin zone. w_k is the fractional weight of k-point k. c is the plane wave expansion coefficient. The plane wave coefficients for all orbitals ($c_{(\vec{G}+\vec{k}),m}$ and $c_{\vec{G}',l}$) are calculated using DFT. $\vec{G}$ and $\vec{G}'$ are plane wave basis sets for the orbitals m and l, respectively. $\vec{r}$ is a position vector within the periodic unit cell. Equation (2) simplifies to Eq. (3) (below) when we impose the orthonormality condition on the plane waves. For simplicity, we use the same plane wave basis sets for both the interacting and isolated systems ($\{\vec{G}\}=\{\vec{G}'\}$):

$$\mathrm{PDOS}(l,E)=8\pi^3\sum_m \left| \sum_k w_k \sum_p c^*_{(\vec{G}+\vec{k}),m} c_{(\vec{G}+\vec{k}),l} \right|^2 \times \delta(E-E_{m,k}). \quad (3)$$

For an atomic level interacting with a continuum of surface levels, the PDOS is a Lorentzian with width Γ. To extract the width Γ from Eq. (3), we self-convolute Eq. (3) with a Lorentzian of width β. The effect is simply to approximate the δ function in Eq. (3) with a Lorentzian [Eq. (4)]:

$$\delta(E-E_m)\cong \frac{\beta/2\pi}{(E-E_m)^2+(\beta/2)^2}. \quad (4)$$

The resulting PDOS is now a Lorentzian of width $\Gamma(\beta)=\Gamma+\beta$. The atomic level width is obtained from $\Gamma=\Gamma(\beta)-\beta$. Since the PDOS is only sampled at discrete energies E_m, our calculated PDOS will not be perfectly Lorentzian. Therefore, Γ depends on the choice of the arbitrary β parameter. In practice, Γ depends only weakly on β and we find the optimal β, β_{opt}, by choosing the value where Γ is stationary and continuous, i.e., where $d\Gamma/d\beta=0$. The optimal value of gamma, $\Gamma(\beta_{\mathrm{opt}})$, is the energy level width associated with the orbital onto which we project in Eq. (1). By repeating this process for different atom-metal surface distances, we determine the energy level width as a function of distance.

For the time-independent case, the broadening Γ is inversely related to the instantaneous lifetime as $\Gamma=\hbar/\tau$. If the atom was stationary, then this instantaneous lifetime τ would be directly proportional to the charge-transfer rate. However, since the atom is moving, this relationship $\Gamma=\hbar/\tau$ no longer correctly accounts for the charge transfer. Instead, a dynamical Hamiltonian must be used to relate the broadening (Γ_{opt}) to the charge-transfer probability, as described later.

III. DFT CALCULATIONAL DETAILS

To model the periodically infinite metal crystal surface, we use the plane wave pseudopotential DFT code CASTEP.[12] The LDA is employed to account for electron exchange and correlation. Trouiller-Martins norm-conserving nonlocal pseudopotentials[16] are used to replace the effect of the nuclei and core electrons in both Al and Li. Use of a pseudopotential for Li allows the Li $2s$ electron to be treated within the one-orbital PDOS formalism described in Sec. II. The local (p) and s channels of the Li pseudopotential both utilize a pseudization radius of 2.432 bohrs, with a nonlinear core correction radius of 1.294 bohrs. For aluminum, the local (d), s, and p channels, all utilize a pseudization radius of 2.276 bohrs, with a nonlinear core correction radius of 1.110 bohrs. This pseudopotential for Al, when used with a converged basis, yields a lattice constant of 7.532 bohrs and a bulk modulus of 73 GPa for bulk Al. Experimental results, extrapolated to zero kelvin,[17] deviate from these values by $\sim$1% for the lattice constant and $<$5% for the bulk modulus. A kinetic energy cutoff of 500 eV for the plane wave basis expansion is used to attain accuracy in the total energy of $\sim$0.002 eV/atom. Our method for predicting the level widths is extremely sensitive to k-point density; a k-point lateral spacing of 0.0237 bohrs^{-1} properly converges our calculations.

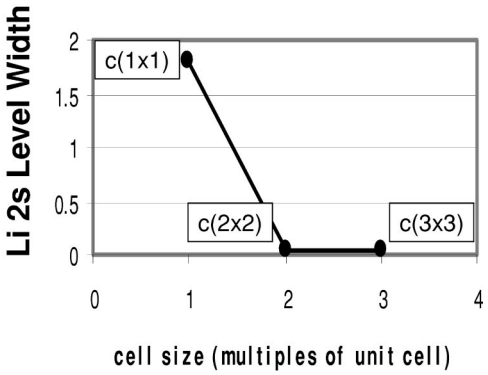

FIG. 1. Cell size effect on broadening. Absorbate level width converges rapidly with lateral cell size. The Al(001)-$c(2\times2)$ surface unit cell is sufficiently converged to determine the widths.

The semi-infinite Al(001) metal surface is approximated by a periodic unit cell consisting of 19 bohrs of vacuum and containing a sufficient number of atomic layers to properly mimic the crystalline surface. In order to model an isolated atom-surface scattering event, we also systematically increase the lateral unit cell from the four-atom fcc surface unit cell until convergence of the Li $2s$ level width is achieved. Figure 1 displays how the widths change as the Li-Li distance in neighboring cells is increased for a Li atom 7 bohrs above the Al(001) surface represented by a thin three-layer slab. We see that the Li atom is effectively isolated from its periodic images by the point at which they are 15 bohrs apart in the $c(2\times2)$ cell containing eight atoms per layer. Slight differences in widths between the $c(2\times2)$ and the $c(3\times3)$ cells appear to be due to higher Li-induced surface polarization in the $c(2\times2)$ cell, as seen in the Al local density of states (not shown). In addition to requiring at least eight atoms per surface layer, we found that convergence of the energy level widths requires at least seven layers of atoms in the slab (see Fig. 2). We also found that relaxation of the bulk-terminated Al(001) slab results in $<$1% change in the

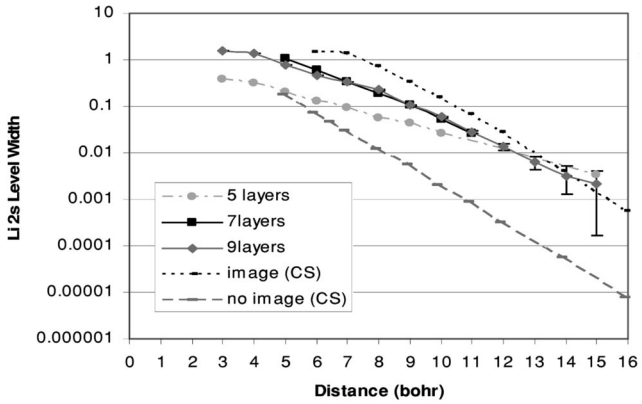

FIG. 2. Convergence of Li $2s$ level widths as a function of Al(001) slab thickness. The widths Γ of the Li $2s$ level are essentially converged by seven layers. The complex scaling (CS) predictions with and without the image potential bound the DFT results. The error bars shown represent $+/-0.002$ eV estimates of residual numerical error in the DFT calculations.

interlayer spacing. In all calculations reported below, the unrelaxed Al(001)-$c(2\times2)$ nine-layer slab was employed. Last, the work function Φ of Al was calculated within DFT, via the relation $\Phi=\epsilon_{\mathrm{vac}}-\epsilon_f$, the difference in energies between the vacuum and Fermi levels. The vacuum energy level was calculated directly from the KS electrostatic potential of the Al slab at long range.

IV. ANALYSIS OF ENERGY LEVEL WIDTHS

The calculated energy level widths (solid gray line) for a nine-layer slab are shown in Fig. 2. For comparison we also show results obtained using the complex scaling method[2] (dotted black line) based on a jellium description of the Al surface. We also include results calculated using a finite barrier model (dashed gray line) of the surface, which neglects the image force.[18] The image potential reduces the potential barrier between the surface and the atom, consequently increasing the atomic energy level widths.[18] As a result, the finite barrier predictions are one to two orders of magnitude lower than the complex scaling theory predictions. The error bars illustrate the estimated maximum plane wave basis error of 0.002 eV. Note that finite numerical error associated with the plane wave DFT method (Sec. III) only becomes problematic at larger distances where the magnitudes of the energy level widths themselves approach the numerical error of the calculation. For the purpose of the application to low-energy Li^+ scattering, these numerical errors have a negligible effect on the neutralization probability due to their small magnitude. The accuracy of our widths can be improved by increasing the DFT kinetic energy cutoff and k-point sampling, but at an exorbitant computational cost. For distances closer to the surface, our results are markedly different from the complex scaling predictions, undoubtedly due to the improved description of the atomistic chemical interaction between the atom and the surface not accounted for within the jellium potential used in the complex scaling calculations.

Further analysis of the chemical interactions provides an explanation for the short-range deviations from complex scaling theory. At close Li-Al(001) distances, the Li $2s$ orbital strongly hybridizes with the Al metal valence electrons, broadening the $2s$ energy level. A qualitative measure of the Li-Al(001) hybridization (ρ_{hyb}) as a function of distance can be estimated from the difference between the density of the interacting Li/Al(001) system (ρ^{int}) and the sum of the densities of the isolated Al surface (ρ^0_{Al}) and the Li atom (ρ^0_{Li}), $\rho_{hyb}=\rho^{\mathrm{int}}-\rho^0_{\mathrm{Al}}-\rho^0_{\mathrm{Li}}$. Figure 3 shows this hybridization estimate as a function of Li-Al(001) distance for both the on-top

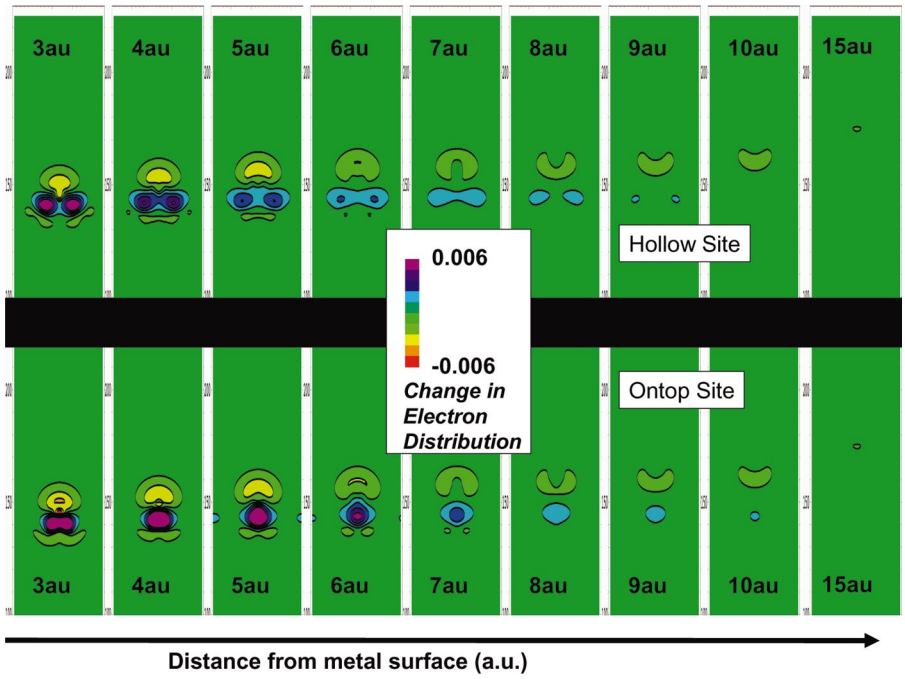

FIG. 3. (Color) Hybridization as a function of Li-Al(001) distance. The hybridizations (changes in electron distribution) decrease as the Li-Al(001) distance increases. These hybridizations are directly related to the Li $2s$ energy level widths.

and the hollow sites of Al(001). The purple color indicates a maximum increase in electron density and red indicates a maximum decrease. As expected, the strength of the hybridization decreases as the Li-Al(001) distance increases. These results corroborate Fig. 2 by showing at small distances that hybridization is quite significant, leading to nontrivial deviations from complex scaling predictions. However, at larger Li-Al(001) distances, the hybridization effects are minute, resulting in asymptotic convergence to jellium-based complex scaling predictions for both sites.

At large distances, the image potential is not accurately modeled by the LDA. The effect of the image potential on the width of the atomic levels outside a metal surface is somewhat complicated. There are two contributions to the image potential for a valence electron of an alkali metal atom outside a metallic surface: the attraction of the electron to its own surface image and the repulsion of the electron to the image of its atomic core.

The attractive interaction, which lowers the barrier to neutralization, is not well described by the LDA exchange-correlation potential, which vanishes exponentially rather than as $-1/4z$. LDA therefore overestimates the potential barrier for resonant neutralization, resulting in smaller widths. An extreme limit is given by the finite barrier model (see Fig. 2 of Ref. 18), which severely overestimates the potential barrier for resonant neutralization. The consequences of this are shown in Fig. 2, where the energy level widths obtained using the finite barrier are orders of magnitude too low.

The repulsive interaction between the electron and the negative image of the Li core increases the potential energy barrier for resonant neutralization. Underestimating this effect as LDA does leads to an increased resonant neutralization rate.[19] Therefore, the LDA errors in treating the two effects compensate for each other. In the application presented below, charge transfer occurs at relatively small Li-Al(001) distances where LDA may provide a reasonable description of the image effects. Future work will improve upon the present LDA-DFT by including exact exchange and more accurate correlation via an embedding theory.[20,21]

V. DYNAMICAL THEORY

The charge transfer in an atom-surface scattering event can be described using the time-dependent Anderson Hamiltonian

$$H(t)=\sum_l \epsilon_l(\vec{R}[t])n_l+\sum_{l\neq l'} U_{ll'}n_l n_{l'}+\sum_k \epsilon_k n_k + \sum_{kl} V_{lk}(\vec{R}[t])c_l^+ c_k+\sum_{kl} V_{kl}(\vec{R}[t])c_k^+ c_l, \quad (5)$$

where ϵ_l are the energy levels of the impinging atom, $n_l\,(n_k)$ are the energy levels of the atom (metal), $\vec{R}[t]$ is the trajectory of the atom, $U_{ll'}$ are the gaseous atom's intra-atomic Coulomb energies, ϵ_k are the energy levels of the metal surface, V_{lk} are the hopping matrix elements between the atom state l and metal state k, and c_l^+ and c_k are the electron creation and annihilation operator for states l and k, respectively. This Hamiltonian is solved using the noncrossing approximation[22] via a nonequilibrium Green's function method.[13]

The input parameters in this approach are the atomic level energy shifts and widths (Sec. II), the work function of the metal, the trajectory of the atom, the surface temperature (300 K), and the half width of the surface conduction band [11.7 eV for Al(001)]. The trajectory of the atom is determined by the exit velocity v (670 eV kinetic energy[14]) and the scattering angle (30°–90°). The initial position of the atom is 2.5 bohrs above the surface, a position at which the Li $2s$ level is fully above the Al Fermi level and hence the Li may be considered fully ionized. The shifts of the Li $2s$ level are not easily extracted from the periodic DFT calculations due to the hybridization effects at short distances that spread the energy level and make it hard to define the shifts unambiguously. Instead, here we employ the same shifts calculated in the complex scaling theory, which essentially follow the classical image potential and can be calculated accurately using first-order perturbation theory. The Al work function is used in the calculation of the energy level shifts to establish a common baseline for the Fermi level of Al. The DFT calculated work function of 4.26 eV for a clean Al(001)-$c(2\times2)$ nine-layer slab is similar to the experimental result of 4.41 eV.[23] However, we find that the DFT work function is sensitive to the thickness of the slab chosen to represent the bulk crystal, decreasing by 0.09 eV as the thickness goes from seven to nine layers. As we will see, small changes in the work function can shift the Li^+ neutralization fractions significantly.

VI. NEUTRALIZATION OF Li^+ SCATTERING AGAINST Al(001)

In order to simulate the scattering event, we first equilibrate the Li atom close to the surface using Eq. (5). As mentioned above, we find that at 2.5 bohrs, after equilibration, the Li atom is fully ionized, so this distance is used as the starting point for the trajectory. The results do not depend on the starting point as long as the initial population of the $2s$ level is relatively small. Then the Li^+ ion is allowed to move linearly away from the surface at a given effective exit angle Θ. Only the perpendicular component of the exit velocity, $\mathbf{v}\sin\Theta$ enters the charge-transfer model. The charge-transfer rate peaks when the Li $2s$ level crosses the Al(001) Fermi level at $\sim$8 bohrs from the surface and the charge transfer ceases $\sim$14 bohrs away from the surface. In other words, at distances of at least 14 bohrs, the energy level widths are too small to allow noticeable charge transfer for the 30°–90° exit angle trajectories investigated here.

We compare now our DFT-based method and complex scaling theory to experimental data from Weare and Yarmoff.[14] Figure 4 shows the predicted fractions of 670 eV Li^+ ions that neutralized after scattering off an Al(001) surface, as a function of exit angle from the surface plane. We show predictions from (a) complex scaling widths (dashed lines) using the measured work function of 4.41 eV,[23] (b) our DFT-based widths (solid lines) using the experimental work function, the DFT work function, as well as one adjusted to give the best agreement to experiment. The energy level

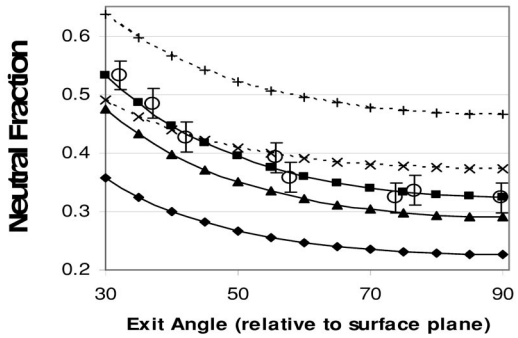

FIG. 4. Fraction of neutralized ions as a function of exit angle, for 670 eV $^7Li^+$ scattering from clean Al(001). Complex scaling (dashed lines; "×," Φ=4.41 eV and "+," Φ=4.26 eV) fails to describe the dependence on exit angle, whereas the DFT widths (solid lines; squares Φ=4.18 eV, triangles Φ=4.26 eV, and diamonds Φ=4.41 eV) yield the correct exit angle trend. Experimental data (open circles) are from Weare and Yarmoff (Ref. 14). Note the sensitivity of the results to the choice of the work function Φ that sets the position of the metal Fermi level.

widths for the on-top site and the hollow site were similar enough that a negligible surface corrugation effect (less than 5%) was observed for the 30°–90° exit angle scattering, therefore only widths calculated from the on-top site were used in the dynamics.

While the complex scaling calculations using the experimental work function (dashed line) roughly obtain the correct magnitude of the neutralization fractions, the complex scaling predictions fail to describe the significant dependence of the neutral fraction on exit angle. On the other hand, the DFT-based predictions of the dependence of the neutralization fractions on exit angle are quite similar to those observed experimentally. However, our predicted neutral fractions using the DFT work function of 4.26 eV (black triangles) are lower than those measured; use of the experimental work function simply worsens the agreement further. As we know, the neutral fractions depend strongly on the relative positions of the Li 2*s* level and the Fermi level of the metal. The black squares show the results obtained assuming a work function of 4.18 eV, which produces almost perfect agreement with experiment. A decrease of the work function in our model for charge transfer is physically equivalent to a downward shift of the Li 2*s* level or a corresponding upward shift in the Fermi level of the Al. It is not unreasonable to expect that the hybridization between the Li 2*s* and the Al surface could induce such shifts equivalent to the 0.08 eV Fermi energy difference between the black lines.

VII. CONCLUSIONS

A recently developed quantum chemical approach for calculating energy level widths of atomic species outside metal clusters was extended to periodic slab models of a metal surface. The method was applied to the Li 2*s* level outside an Al(001) surface. We explicitly showed that hybridization between Li 2*s* level and Al surface energy levels correlates with broadening of the Li 2*s* level as it approaches the surface. The hybridization is a chemical interaction not described by the conventional jellium approaches. Our method directly calculates the atomic energy level widths from a periodic density functional theory description of the metal surface. Then, neutralization fractions are predicted via an Anderson Hamiltonian using our energy level widths to define charge-transfer rates between the ion and the metal surface. This combined periodic DFT/dynamics approach yields the correct dependence of neutralization fractions on ion exit angles for this system,[14] while jellium-based models do not. Not surprisingly, the absolute magnitude of the neutralization fractions is found to depend very sensitively on the metal work function and hence on the actual energy level shifts employed. The next stage of this work is to develop the means to calculate reliable energy level shifts from first principles so that the scattering problem can be defined completely within an *ab initio* model via both widths and shifts of atomic energy levels near metal surfaces calculated from first principles.

ACKNOWLEDGMENTS

We thank the National Science Foundation and the Robert A. Welch Foundation (Grant No. C-1222) for supporting this work, Hewlett-Packard for donating the Itanium computers used in this work to the California NanoSystems Institute (CNSI), Professor Jory Yarmoff (UC Riverside) for insightful discussions, and Dr. Niranjan Govind (Accelrys, Inc.) for assistance with CASTEP.

[1] H. Winter, Phys. Rep. **367**, 387 (2002).
[2] P. Nordlander and J. C. Tully, Phys. Rev. Lett. **61**, 990 (1988).
[3] D. Teillet-Billy and J. P. Gauyacq, Surf. Sci. **239**, 343 (1990).
[4] P. Kürpick and U. Thumm, Phys. Rev. A **58**, 2174 (1998).
[5] C. C. Hsu, H. Bu, A. Bousetta, J. W. Rabalais, and P. Nordlander, Phys. Rev. Lett. **69**, 188 (1992).
[6] E. C. Goldberg, R. Monreal, F. Flores, H. H. Brongersma, and P. Bauer, Surf. Sci. **440**, L875 (1999).
[7] A. G. Borisov, A. K. Kazansky, and J. P. Gauyacq, Surf. Sci. **430**, 165 (1999).
[8] A. G. Borisov, A. K. Kazansky, and J. P. Gauyacq, Phys. Rev. Lett. **80**, 1996 (1998).
[9] M. Taylor and P. Nordlander, Phys. Rev. B **64**, 115422 (2001).
[10] W. More, J. Merino, R. Monreal, P. Pou, and F. Flores, Phys. Rev. B **58**, 7385 (1998).
[11] W. Kohn and L. J. Sham, Phys. Rev. **140**, 1133A (1965).
[12] M. C. Payne, M. P. Teter, D. C. Allan, T. A. Arias, and J. D. Joannopoulos, Rev. Mod. Phys. **64**, 1045 (1992).
[13] H. X. Shao, D. C. Langreth, and P. Nordlander, Phys. Rev. B **49**, 13929 (1994).
[14] C. B. Weare and J. A. Yarmoff, Surf. Sci. **348**, 359 (1996).
[15] A. G. Borisov, G. E. Makhmetov, D. Teillet-Billy, and J. P. Gauyacq, Surf. Sci. **375**, L367 (1997).
[16] N. Troullier and J. L. Martins, Phys. Rev. B **43**, 1993 (1991).
[17] G. N. Kamm and G. A. Alers, J. Appl. Phys. **35**, 327 (1964).
[18] P. Nordlander, Phys. Rev. B **53**, 4125 (1996).
[19] P. Nordlander and J. C. Tully, Phys. Rev. B **42**, 5564 (1990).
[20] T. Kluner, N. Govind, Y. A. Wang, and E. A. Carter, Phys. Rev. Lett. **86**, 5954 (2001); J. Chem. Phys. **116**, 42 (2002); Phys. Rev. Lett. **88**, 209702 (2002).
[21] N. Govind, Y. A. Wang, A. J. R. da Silva, and E. A. Carter, Chem. Phys. Lett. **295**, 129 (1998); N. Govind, Y. A. Wang, and E. A. Carter, J. Chem. Phys. **110**, 7677 (1999).
[22] N. E. Bickers, Rev. Mod. Phys. **59**, 845 (1987).
[23] J. K. Grepstad, P. O. Gartland, and B. J. Slagsvold, Surf. Sci. **57**, 348 (1976).